First-principles calculation of H vibrational excitations at a dislocation core of Pd

Hadley M. Lawler and Dallas R. Trinkle[*]

Department of Materials Science and Engineering, University of Illinois, Urbana-Champaign, 1304 W. Green St., Urbana, IL 61801 USA
(Received 6 August 2010; published 18 November 2010)

Palladium is an ideal system for understanding the behavior of hydrogen in metals. In Pd, H is located both in octahedral sites and in dislocation cores, which act as nanoscale H traps and form Cottrell atmospheres. Adjacent to a dislocation core, H experiences the largest possible distortion in α-Pd. *Ab initio* density-functional theory computes the potential energy for a hydrogen in an octahedral site in α-Pd and in a trap site at the core of a partial of an edge dislocation. The Pd partial dislocation core changes the environment for H, distorting the H-Pd bonding which changes the local potential, vibrational spectra, and inelastic form factor for an isolated H atom. The decrease in excitation energy is consistent with experiments, and the calculations predict distortions to the H wave function.

Renewable energy requires new methods for the production, storage, and transportation of energy from the point of production. The potential for hydrogen as an energy storage medium[1] has renewed interest in the fundamentals of hydrogen in metals—a topic with a long history.[2] In particular, the ease of catalysis of molecular to atomic hydrogen on the surface of palladium has motivated the study of atomic hydrogen and hydride formation in Pd. Hydrogen's vibrational excitations in metals provide an interesting window into H behavior due to its low mass; and α-Pd is a useful system that is simple to prepare.[3] There are various means of measuring the vibrational energies, such as conductance spectroscopy,[4] Raman scattering,[5] and inelastic neutron scattering.[6] Neutron scattering measured isotopic effects,[7] linewidths, and their dependence on temperature,[8] the optical band, and its high-energy features,[9] and concentration dependence of the spectra.[10] Heuser *et al.*[11] recently measured the hydrogen excitation peak at 4 K to be 59 meV for the dilute (0.08 at. %) H concentration while at 300 K the peak was 68 meV. The low concentration suggests hydrogen trapped at edge-dislocation core interstitial sites. This is due to the strong interactions of dislocations and hydrogen,[12] with a binding energy of 0.2 eV.[13] To determine the effect of the dislocation core on hydrogen vibration spectra, we compute the anharmonic H potential energy adjacent to a dislocation core from first-principles, and calculate excitation energies and wave functions. The result is a decrease in excitation energy consistent with experiments and distortions in the hydrogen wave functions due to strain and symmetry breaking.

The anharmonic potential for hydrogen in Pd increases vibrational excitation energies and produces anisotropy in the inelastic form factor compared with a harmonic potential.[14,15] The low mass of H produces zero-point motion of 0.15 Å in an octahedral interstitial environment in α-Pd, which in turn samples a potential-energy surface that is no longer purely harmonic. This increases transition energies for H vibration in Pd by ∼50% relative to the harmonic approximation.[14] The vibrational spectrum for H has the degeneracy of an octahedral potential,[16] and excitations which are not simple multiples of the first excitation energy.[10] The wave functions have cubic symmetry, and variations in the inelastic form factor with scattering wave vector show modulations between high-symmetry directions.[17,15] How-ever, when a hydrogen atom occupies an octahedral site near a dislocation core, the cubic symmetry is completely broken, and H experiences a distorted environment.

Predicting the vibrational excitations for a hydrogen atom requires accurate computation of the potential energy for hydrogen. Density-functional theory calculations are performed with VASP (Refs. 18 and 19) using a plane-wave basis with the projector augmented-wave (PAW) method,[20] with potentials generated by Kresse.[21] The local-density approximation as parametrized by Perdew and Zunger[22] and a plane-wave kinetic-energy cutoff of 250 eV ensures accurate treatment of the potentials. The PAW potential for Pd treats the *s* and *d* states as valence, and the H *s* state as valence. The restoring forces for H in Pd change by only 5% compared with a generalized gradient approximation, or including Pd 4*p* states in the valence; our choice of the local-density approximation is computationally efficient, and gives an α-Pd lattice constant of 3.8528 Å compared with the experimentally measured 3.8718 Å. To compute the dynamical matrix for the lattice Green's function,[23] and to relax H at the octahedral site in α-Pd, we use a $4 \times 4 \times 4$ simple-cubic supercell of 256 atoms, with a $6 \times 6 \times 6$ *k*-point mesh while the dislocation geometry with 382 atoms uses a $1 \times 1 \times 8$ *k*-point mesh. The electron states are occupied using a Methfessel-Paxton smearing of 0.25 eV. For the H octahedral site in α-Pd and the partial dislocation core, atom positions are relaxed using conjugate gradient until the forces are less than 5 meV/Å.

First-principles calculations using lattice Green's function-based flexible boundary conditions compute a stress-free edge dislocation in Pd. Flexible boundary conditions embed a dislocation in an infinite bulk which responds harmonically to forces.[24,25] The harmonic response is captured by the lattice Green's function, which gives the displacement field necessary to relax a line-force in an infinite harmonic crystal; it is computed directly from the force-constant matrix.[23] The initial geometry is a periodic "slab" supercell of 382 fcc Pd atoms: an infinite cylinder with free surfaces along the dislocation threading line $\frac{a}{2}[1\bar{1}2]$ in a $9a[110] \times 11\frac{a}{2}[\bar{1}11]$ box. Anisotropic elasticity gives the initial displacements for an $\frac{a}{2}[110]$ edge dislocation centered in the cylinder. Flexible boundary conditions use forces from
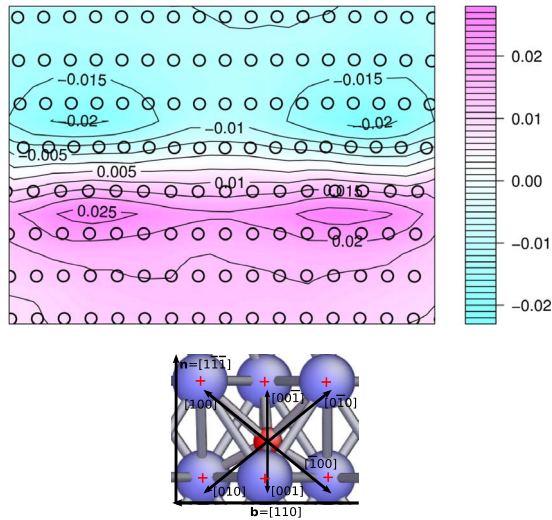
FIG. 1. (Color online) (top) Strain at octahedral sites in Pd edge-dislocation core. The edge dislocation has a total Burgers vector $\frac{a}{2}[110]$ while the partials have Burgers vector $\frac{a}{6}[211]$ and $\frac{a}{6}[12\bar{1}]$ and are separated by $6.5b$. (bottom) Hydrogen (small red) in the octahedral site below the Pd partial dislocation core in the $(1\bar{1}1)$ slip-plane. The hydrogen is in an octahedral site with large tensile strain; the top three Pd atoms are the most expanded, and the bottom three are less expanded. The dislocation core displaces the neighboring Pd atoms for the octahedral site from the relaxed bulk positions shown by the ⟨100⟩ arrows. Moreover, the hydrogen atom moves away from the top three atoms ([100], [00$\bar{1}$], and [0$\bar{1}$0]) increasing the distance to 1.96–2.16 Å. The hydrogen moves closer to the other three atoms, decreasing the distance to 1.87–1.91 Å, compared to a distance of 1.96 Å for H in an octahedral site in fcc-Pd.

density-functional theory, and relaxes each atom based on its location within one of three different regions determined by the distance from the dislocation core.[24,25] The 45 atoms around the core start with nonzero forces, and conjugate-gradient minimization relaxes them while the other atoms are fixed. The neighboring 100 atoms between the core and the free surfaces act as a coupling region to a virtual infinite bulk. They start with zero forces but displacing the core atoms induces forces. With the lattice Green's function, we can displace all 382 Pd atoms to relax the forces in the coupling region. This includes the outer 237 atoms that have nonzero forces due to their proximity to the free surfaces; their forces are ignored in the calculation. The relaxation cycle continues alternating between conjugate gradient near the core and lattice Green's function relaxation in the intermediate region, until all forces are less that 5 meV/Å. The final result is the stress-free dislocation core equilibrium geometry: an edge dislocation split into two $\frac{a}{6}\langle 211 \rangle$-type partials separated by a distance of $6.5b$ (cf. Fig. 1).[26]

Figure 1 shows the distorted local environment for a hydrogen atom adjacent to a partial dislocation core. Interstitial atoms favor regions of expansion, and below the slip plane of the partial dislocation core has maximum tensile strain and nonvolumetric effects, such as differences in the bond lengths along the slip-plane normal. Considering the plane $(1\bar{1}1)$ halfway between the three Pd atoms above and below,

the H atom is displaced away from the partial core (above the top three atoms). The three Pd atoms above the interstitial site have longer Pd-H bond lengths than the three below it. For an idealized edge-dislocation, the slip-plane normal points along the strain gradient from compressive to tensile, and just below the slip plane the predominant strain is uniaxial tension along the Burgers vector. Changes in the bond length above and below the interstitial site are greatest for the [100] and [010] octahedral axes, which are nonorthogonal to the Burgers vector. This effect is such that although there is an overall 5% volume expansion about the interstitial site, the [100] and [010] octahedral axes expand by an average of 3%, and the [001] axis contracts by 2%. For the octahedral axes nonorthogonal to the Burgers vector, there are expansion and contraction of Pd-H bond lengths above and below the interstitial site while bond lengths along the [001] are approximately the same.

The potential energy for H in an octahedral site in α-Pd and a partial dislocation core are fit to force versus displacement data for the hydrogen atom from its relaxed position. Displacements of 0.025, 0.15, and 0.2 Å provide data of restoring force on H, where the 0.025 Å displacements give the harmonic limit and the larger displacements provides information about the anharmonic terms. For α-Pd and α-Pd with a 5% expansion in volume, all small displacement directions are equivalent; we use [100], [110], and [111] directions for 0.2 Å displacements for a total of four displacements. For the partial dislocation core, cubic symmetry is broken: we use all six ⟨100⟩ small displacements and six ⟨100⟩, twelve ⟨110⟩, and eight ⟨111⟩ displacements for a total of 58 displacements. The potential is represented as a fourth order polynomial in displacements x_i; excluding linear and constant terms, this gives 31 terms to be fit (reducing to three in the case of cubic symmetry). This representation of the potential reproduces the first-principles forces to less than 1 meV/Å.[27]

Figure 2 shows that potentials along directions of the shortened bond lengths are steeper than α-Pd while those along elongated bond lengths are shallower. For an octahedral site in α-Pd, the ⟨100⟩ directions are the stiffest while the ⟨111⟩ and ⟨110⟩ directions are shallower. The ⟨110⟩ directions connect neighboring octahedral sites and ⟨111⟩ pass through an octahedral face. All of the potentials soften with the expansion of the lattice by 5%. The softest of the ⟨100⟩-type directions have components along the Burgers vector, and are above the interstitial site, i.e., [100] and [0$\bar{1}$0]. The resultant potential for coordinates along these directions has large cubic terms, reflecting bond-length variation above and below the interstitial site. The potential for the [001] coordinate is less cubic, consistent with the smaller change in bond length along this direction. The distortions to the potential from the dislocation core geometry is reflected in the broken symmetry for excitations and the resulting wave functions for the hydrogen atom.

Table I shows that the predicted transition energies from our potentials; it is an overestimate compared to experimentally measured peaks in scattering intensity but the reduction in transition energy matches well. To solve for the energy spectrum of our potential, we use a basis of products of
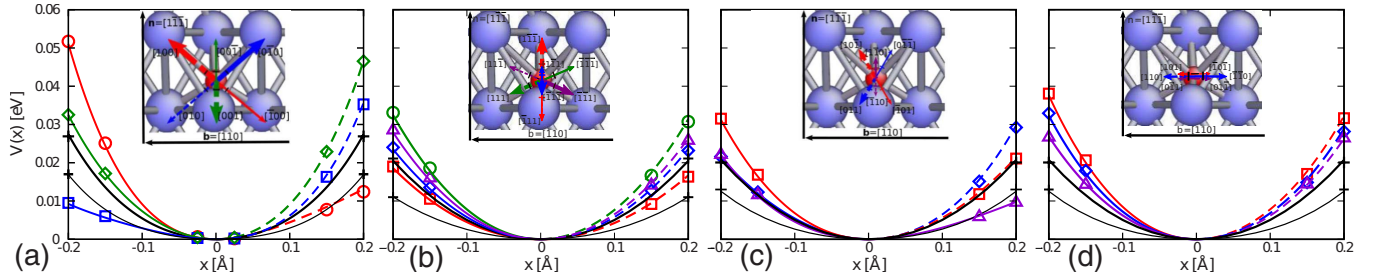
FIG. 2. (Color online) Hydrogen potential energy as a function of displacement along (a) $\langle 100 \rangle$, (b) $\langle 111 \rangle$, (c) $\langle 110 \rangle$ directions in the slip plane, and (d) $\langle 110 \rangle$ directions out of the slip plane. Thick black shows response in α-Pd, and thin black shows response in 5% expanded α-Pd. Positive (negative) displacements along corresponding directions are dashed (solid). Arrows show corresponding displacements, for the potential curves of the same color and linestyle. Thick displacement arrows have positive out-of-page components; negative for thin arrows. Single points on the plots are the results of individual first-principles calculations, and the continuous curves are fit to the Hellmann-Feynman forces. (a) The cube directions [100] (circles), [010] (squares), and [001] (diamonds) show the greatest change to the potential due to the dislocation core. The softest directions, [100] and [0$\bar{1}$0], point toward regions of expansion while the [$\bar{1}$00] and [010] stiff directions bring the hydrogen closer to Pd atoms. (b) The octahedral directions [111] (circles), [$\bar{1}$11] (squares), [1$\bar{1}$1] (diamonds), and [11$\bar{1}$] (triangles) show less change due to the dislocation core. The most significant softening is for the octahedral direction corresponding to the slip-plane normal. (c) The out-of-plane closed-packed directions [10$\bar{1}$] (squares), [011] (diamonds), and [$\bar{1}$10] (triangles) are similarly softened in the direction of expansion and stiffened in the opposite direction compared with bulk. (d) The in-plane closed-packed directions [101] (squares), [110] (diamonds), and [0$\bar{1}$1] (triangles) are all stiffened compared with bulk.

Hermite polynomials in the three displacement directions x_i with a fundamental length x_0. The fundamental length is chosen to harmonically match the anharmonic potential: the harmonic ground state $|000\rangle$ is the solution to a one-dimensional harmonic potential with stiffness $\langle 000|\nabla^2 V|000\rangle/3$. For α-Pd, $x_0 = 0.215$ Å and for a partial dislocation core $x_0 = 0.210$ Å; note that these are larger than the anharmonic ground-state rms spread. The full basis $|m_1 m_2 m_3\rangle$ contains all m_i up to $m_1 + m_2 + m_3 \leq M$, for a total of $(M+3)(M+2)(M+1)/6$ basis functions. Energies for the first three excited states are converged to 0.3 meV with $M=8$ (165 basis functions) and 0.03 meV with $M=16$ (969 basis functions). Our overestimation of the transition energies is consistent with other density-functional theory calculations for the octahe-

TABLE I. Calculated and measured transition energies for H in α-Pd and adjacent to a partial dislocation core. Hydrogen occupies an octahedral site in α-Pd; the transition from the ground state to the triply degenerate first excited state is larger than the experimentally measured peak. A volumetric expansion of 5% reduces the predicted transition energy by 9 meV. The partial dislocation core produces a similar volumetric expansion, but includes additional distortion that lift the degeneracy of the first excited state, giving a set of three low-lying transition energies. The labels $\vec{n}_i$ correspond to the different orientations of the excited-state wave function.

	Theory (meV)	Experiment (meV)
α-Pd	87	69[a]
α-Pd ($\varepsilon_V = 5\%$)	78	
$\vec{n}_1$	56	
$\vec{n}_2$	80	59[b]
$\vec{n}_3$	102	

[a]Reference 10.

[b]Reference 11.

dral site in α-Pd;[28] it is also independent of the exchange-correlation potential and treatment of the ionic cores. The reduction in excitation energy of 7 meV in the dislocation core corresponds with the experimental measurement of 10 meV.

Cubic symmetry is broken at the partial dislocation core, which splits the degeneracy of the excited state, and gives three principal axes for the ground-state wave function spread. The eigenvectors of the spatial covariance matrix, $X_{ij}^{(2)} = \langle x_i x_j \rangle - \langle x_i \rangle \langle x_j \rangle$, give the directions of maximum and minimum spread. The ground-state eigenvectors are $\vec{n}_1 = [0.66, -0.75, -0.06]$, $\vec{n}_2 = [0.73, 0.66, -0.16]$, and $\vec{n}_3 = [0.16, 0.06, 0.99]$—roughly, [1$\bar{1}$0], [110], and [001]—with rms values of 0.19, 0.16, and 0.14 Å; compared to 0.15 Å for H in α-Pd. The soft direction $\vec{n}_1 \approx [1\bar{1}0]$ corresponds with the softest of the nearly symmetric direction in the potential [cf. Fig. 2(c), triangles]; the stiffest direction $\vec{n}_3 \approx [001]$ corresponds with the stiffest nearly symmetric direction in the potential [cf. Fig. 2(a), diamonds], and $\vec{n}_2 \approx [110]$ a mutually orthogonal "bulk-like" potential [cf. Fig. 2(d), diamonds]. Moreover, the three directions correspond to the shapes of the first three excited states in Table I.

The first three excited states are p-like, and have maximum spreads along directions which correspond to $\vec{n}_1$, $\vec{n}_2$, and $\vec{n}_3$. The first-excited state has a maximum spread along $[0.68, -0.73, -0.07]$, the second along $[0.71, 0.68, -0.17]$, and the third along [0.15, 0.11, and 0.98]. The magnitudes of maximum spread for each of the three states are 0.35 Å, 0.27 Å, and 0.23 Å, compared to a maximum spread of 0.25 Å for the first-excited state in α-Pd. The expanded volume in the partial dislocation core decreases the transition energy; however, Table I shows degeneracy-splitting due to broken symmetry from the local strain. This strain allows for a low lying transition state $\vec{n}_1$ that is 30 meV below the similar transition in α-Pd, or 20 meV below in the expanded lattice. This is a direct consequence of the hydrogen occupy-

ing a site near the partial dislocation core. Moreover, we expect that vibrations of neighboring Pd atoms—both at finite temperature and from zero-point motion—will lead to broadening of the excitation peaks, and, in particular, exacerbate the symmetry breaking. This should lead to greater broadening of the $\vec{n}_1$ and $\vec{n}_3$ states than the $\vec{n}_2$ states, implying that the broken-symmetry "satellite" excitations may be difficult to observe directly in experiments. Hence, the predicted reduction in excitation energy of 7 meV is consistent with the experimentally measured reduction of 10 meV.

Figure 3 shows the orientation of the first three excited states by plotting the inelastic form factor, $S(\vec{q})$ from the ground state to each excited state. The inelastic form factor, for an excitation from the ground state $|0\rangle$ to excited state $|\vec{n}_i\rangle$, $S(\vec{q})=|\langle 0|\exp(-i\vec{q}\cdot\vec{r})|\vec{n}_i\rangle|^2$ determines the intensity of inelastic scattering with scattering direction $\vec{q}$. In Fig. 3, we rotate $\vec{q}$ from $\vec{n}_1$ to $\vec{n}_2$ to $\vec{n}_3$ and back to $\vec{n}_1$. For comparison, we also compute $S(\vec{q})$ with bulk excited states projected along $\vec{n}_i$. The excited states have similar structure to the excited states in α-Pd site. The changes in inelastic form factors are due to the expansion of the excited state along the $\vec{n}_i$ directions compared with bulk, where expanded wave functions decrease $S(\vec{q})$.

Density-functional theory calculations combined with accurate treatment of boundary conditions compute the relaxed geometry for a hydrogen atom adjacent to a partial dislocation core in Pd. We extract the local potential energy for the hydrogen atom from first-principles to predict the quantum-mechanical transition energies, and compare to the transition energies in an octahedral site in α-Pd. The changes in the excitation energies can be directly traced to the distortions in geometry around the hydrogen atom, the potential energy, and ultimately the wave functions for hydrogen. The predicted decrease due to the volumetric expansion is similar to the change in experimental measurements at low temperatures where the hydrogen occupancy of partial dislocation cores should come to dominate. This provides an important step in understanding the changes in vibrational spectra from
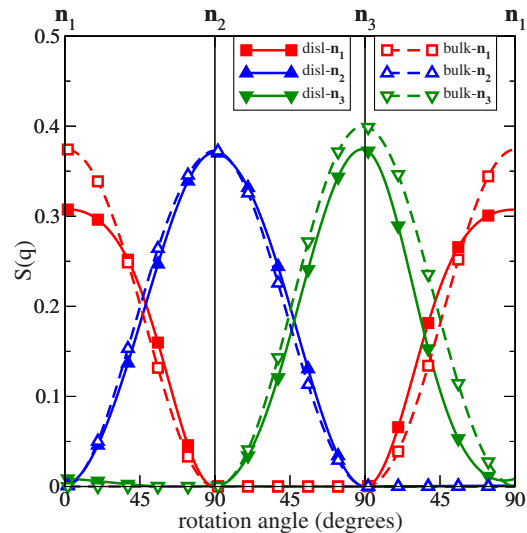

FIG. 3. (Color online) Inelastic form factor $S(\vec{q})$ for a H adjacent to the dislocation core and in octahedral bulk sites. The momentum $\vec{q}$ rotates between the three orthogonal vectors $\vec{n}_i$, corresponding to the directions of maximal ($\vec{n}_1$) and minimal ($\vec{n}_3$) spread of the H ground-state wave function in a dislocation core. The peak along each $\vec{n}_i$ indicates that the excited state is p-like along that direction. The form factors for *bulk* excited states which maximize overlap with the dislocation core states shows a similar peak shape with direction. The height of the peaks corresponds to the spreading of the excited states along those directions in comparison with the ground state: increased spreading of the excited states along the particular direction decreases the peak height.

hydrogen in Pd as temperature changes and the hydrogen atoms migrate to more energetically favorable sites in the sample. In addition, the potential provides a starting point for considering pipe diffusion of H along dislocation cores in Pd.

*dtrinkle@illinois.edu

[1] L. Schlapbach and A. Züttel, Nature (London) **414**, 353 (2001).
[2] S. M. Myers *et al.*, Rev. Mod. Phys. **64**, 559 (1992).
[3] T. B. Flanagan and W. A. Oates, Annu. Rev. Mater. Sci. **21**, 269 (1991).
[4] S. Csonka *et al.*, Phys. Rev. Lett. **93**, 016802 (2004).
[5] R. Sherman *et al.*, Phys. Lett. A **62**, 353 (1977).
[6] W. Drexel *et al.*, J. Phys. Chem. Solids **37**, 1135 (1976).
[7] V. E. Antonov *et al.*, Phys. Rev. B **80**, 134302 (2009).
[8] M. R. Chowdhury and D. K. Ross, Solid State Commun. **13**, 229 (1973).
[9] J. M. Rowe *et al.*, Phys. Rev. B **8**, 6013 (1973).
[10] J. J. Rush *et al.*, Z. Phys. B: Condens. Matter **55**, 283 (1984).
[11] B. J. Heuser *et al.*, Phys. Rev. B **78**, 214101 (2008).
[12] R. Kirchheim, Acta Metall. **29**, 835 (1981).
[13] B. J. Heuser and J. S. King, Metall. Mater. Trans. A **29**, 1593 (1998).
[14] C. Elsässer *et al.*, Phys. Rev. B **44**, 10377 (1991).

[15] M. Kemali *et al.*, Phys. Rev. Lett. **84**, 1531 (2000).
[16] H. Krimmel *et al.*, J. Phys.: Condens. Matter **6**, 7679 (1994).
[17] R. Hempelmann *et al.*, Phys. Rev. Lett. **58**, 1016 (1987).
[18] G. Kresse and J. Hafner, Phys. Rev. B **47**, 558 (1993).
[19] G. Kresse and J. Furthmüller, Phys. Rev. B **54**, 11169 (1996).
[20] P. E. Blöchl, Phys. Rev. B **50**, 17953 (1994).
[21] G. Kresse and D. Joubert, Phys. Rev. B **59**, 1758 (1999).
[22] J. P. Perdew and A. Zunger, Phys. Rev. B **23**, 5048 (1981).
[23] D. R. Trinkle, Phys. Rev. B **78**, 014110 (2008).
[24] J. E. Sinclair *et al.*, J. Appl. Phys. **49**, 3890 (1978).
[25] S. Rao *et al.*, Philos. Mag. A **77**, 231 (1998).
[26] B. J. Heuser *et al.*, in *Effects of Hydrogen on Materials*, Proceedings of the 2008 International Hydrogen Conference (ASM International, Materials Park, OH, 2009), pp. 464–468.
[27] See supplementary material at http://link.aps.org/supplemental/10.1103/PhysRevB.82.172101 for restoring force data and polynomial potential coefficients.
[28] X. Ke and G. J. Kramer, Phys. Rev. B **66**, 184304 (2002).